Electrically tunable photo-aligned two-dimensional liquid crystal polarisation grating

Song-zhen Li, Zhi-Wei Zhao, Cheng-Miao Wang, Qi-dong Wang, Lishuang Yao, Zeng-Hui Peng, Yong-gang Liu & Li Xuan

Published online: 11 Nov 2018.

Submit your article to this journal ⬈

Article views: 14

View Crossmark data ⬈

Taylor & Francis
Taylor & Francis Group

Electrically tunable photo-aligned two-dimensional liquid crystal polarisation grating

Song-zhen Li[a,b], Zhi-Wei Zhao[a,b], Cheng-Miao Wang[a,b], Qi-dong Wang[a], Lishuang Yao[a], Zeng-Hui Peng[a], Yong-gang Liu[a] and Li Xuan[a]

aState Key Laboratory of Applied Optics, Changchun Institute of Optics, Fine Mechanics and Physics, Chinese Academy of Sciences, Changchun, Jilin, China; bSchool of Optoelectronics, University of Chinese Academy of Sciences, Beijing, China

ABSTRACT

Two-dimensional liquid crystal polarisation grating based on twist liquid crystal has been demonstrated and fabricated by polarisation holography in this paper. The maximal diffraction efficiency of the second order is up to 90%. And the two-dimensional liquid crystal polarisation grating has the properties of electrically tenability and polarisation tenability. The two-dimensional polarisation grating diffracts light into a spot array. Different direction diffraction light is with different polarisation states. The intensity of the different orders diffraction light is optically controlled.
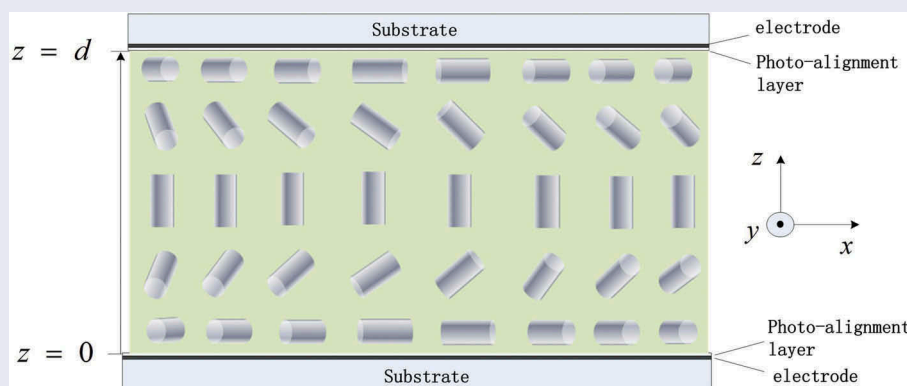
1. Introduction

Liquid crystal (LC)-based diffraction gratings have attracted great interest due to their promising applications in displays technology [1], photonics [2] and optical communication [3]. The high birefringence, high sensitivity to external fields and the influence of the surface anchoring forces allow to develop highly functional optical devices for information technologies [4,5]. Among LC diffraction gratings, LC polarisation grating is a promising element. It employs the Pancharatnam-Berry phase principle and operates on circular eigen-polarisations [6,7]. Specially, liquid crystal polarization grating (LCPG) exhibits high first-order diffraction efficiency and excellent polarisation splitting properties [8–10]. Because of these advantages, their potential applications include polarisation converters [11], laser beam steering [12], Stokes polarimeters [13], optical filters [14] and so on. It is important to control the substrate surface anchoring for the realisation of LC

polarisation grating. Several approaches have been proposed to obtain multi-domain LC films with periodic orientation of the nematic director: photo-lithography [15], digital micro-mirror dynamic microlithography [16], mask photo-polymerisation [17], atomic force microscope patterning [18], polarisation holography [19] and direct-write laser scanning [20]. Among these methods, the polarisation holography is a versatile single step technique that exploits polarisation holograms recorded on the photosensitive aligning layers and has demonstrated spatial modulation of the optical axis direction in the LC bulk.

Polarisation holography makes use of interfering beams of equal intensity and orthogonal linear or circular polarisations to realise a periodic modulation of the light polarisation state in the interference region, where the intensity is almost uniform. In this way, polarisation holography allows a fine and local control of the LC anchoring direction on the polarisation-

sensitive aligning materials. Exploiting this method, LC polarisation grating has been obtained. In the past decade, several groups have been actively engaged in the development of LC polarisation grating. Crawford et al. firstly demonstrated the method of patterning surfaces for LC alignment using a polarisation holography exposure on a photo-polymerisable polymer alignment layer [21]. Komanduri et al. discussed the nature of switching transition threshold for various types of alignment configurations [22]. Subsequently, the bandwidth of LCPG is improved to $\Delta\lambda/\lambda \sim 56\%$ by C. Oh which is based on phase compensation with twisted LC layer [23].

Crawford et al. firstly demonstrated the two-dimensional (2D) LC polarisation gratings by cross assembling two one-dimensional polarisation holography recorded photo-aligning substrates [24]. Subsequently, Provenzano et al. fabricated 2D LC polarisation gratings by the similar way and measured the polarisation property and electrical–optical property [25]. And recently, Mengfei Wang et al. researched the twist disclination lines generated by the 2D LC polarisation grating [26]. Inge Nys et al. analysed the LC superstructures induced by 2D LC grating experimentally by polarising optical microscopy with different applied voltages [27]. The 2D LC gratings diffracted light in 2D directions with different polarisation states. It diffracts incident light into a spot array and can meet the need of manipulating multi-beam optical signal. However, comparing with the traditional polarisation grating, the diffraction efficiency of the 2D polarisation grating is very low, especially for the higher orders. Besides, the theory analysis of the diffraction phenomenon of 2D polarisation grating is still not completed.

In this paper, three 2D polarisation gratings were fabricated with the top and bottom substrates grating vector crossing angles of $\pi/2$, $3\pi/4$ and π, respectively. There are twist deformation in the LC bulk due to crossing angle of grating vectors on the top and bottom

substrate. However, when the 2D polarisation grating is applied with an enough high voltage, the LC molecule in the middle plane aligns vertically to the substrates, and the twist deformation no longer exists in the LC bulk. In the case, the 2D polarisation grating can be considered as a stack of two HAN polarisation gratings [28] with different grating vectors. And the diffraction property of the 2D polarisation grating is obtained by Jones matrix calculation. The diffraction phenomenon of fabricated 2D polarisation grating is consistent with theory analyses. The maximum of the higher order diffraction efficiency is up to 100% theoretically when the phase retardation of the LC cell equals $2N\pi$ (N is an integer). The incident light can be diffracted into several orders with polarisation state turned into circular polarisation.

2. Theory

When the twist LC polarisation grating is applied with an appropriate voltage, the LC molecule of the middle plane aligns vertically to the substrates, and the twist deformation no longer exists in the LC cell, as shown in Figure 1. Under this circumstance, the twist LCs polarisation gratings can operate as a stack of two HAN polarisation gratings [29] with different grating vectors. It functions as a 2D LC polarisation grating.

When the light passes through the 2D polarisation grating, the transmitted light distribution can be calculated by Jones matrix. The LC molecule directors in the top substrate obey the following equation in $x - y$ plane: $\varphi(x) = \pi x/\Lambda$, where Λ is the pitch of the polarisation grating. Its transfer matrix can be expressed as [30]

$$T_1 = R(-\varphi) \cdot \begin{pmatrix} \exp\left(-\frac{i\Gamma}{2}\right) & 0 \\ 0 & \exp\left(\frac{i\Gamma}{2}\right) \end{pmatrix} \cdot R(\varphi)$$

where Γ is the phase retardation $\Gamma = 2\pi\Delta nd/\lambda$, Δn is the LC birefringence, d is the LC cell gap and λ is the
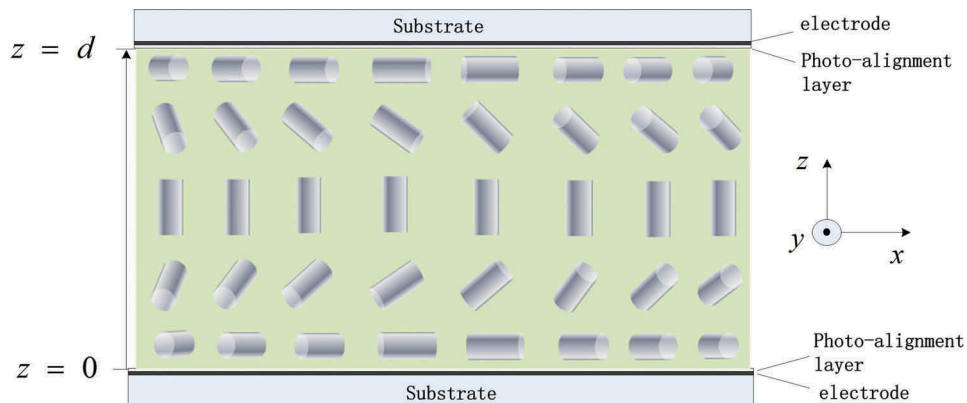

Figure 1. (Color online) LC molecular orientation models of two-dimensional polarisation grating with an external electric field.

free space wavelength. Given the angle between the two grating vectors θ, the LC directors in the bottom substrate obey the equation in $x - y$ plane: $\varphi'(x, y) = \pi(x\cos\theta - y\sin\theta)/\Lambda - \theta$ as shown in Figure 2. Its transfer matrix can be expressed as

$$T_2 = R(-\varphi') \cdot \begin{pmatrix} \exp(-\frac{i\Gamma}{2}) & 0 \\ 0 & \exp(\frac{i\Gamma}{2}) \end{pmatrix} \cdot R(\varphi')$$

The total transfer matrix of the 2D polarisation can be expressed as

$$T = T_2 \cdot T_1$$
$$= \cos^2\left(\frac{\Gamma}{2}\right)\begin{pmatrix} 1 & 0 \\ 0 & 1 \end{pmatrix} - \frac{i}{2}\sin\frac{\Gamma}{2}\cos\frac{\Gamma}{2}e^{i2\varphi}\begin{pmatrix} 1 & i \\ i & -1 \end{pmatrix}$$
$$- \frac{i}{2}\sin\frac{\Gamma}{2}\cos\frac{\Gamma}{2}e^{-i2\varphi}\begin{pmatrix} 1 & -i \\ -i & -1 \end{pmatrix} - \frac{i}{2}\sin\frac{\Gamma}{2}\cos\frac{\Gamma}{2}e^{i2\varphi'}\begin{pmatrix} 1 & i \\ i & -1 \end{pmatrix}$$
$$- \frac{i}{2}\sin\frac{\Gamma}{2}\cos\frac{\Gamma}{2}e^{-i2\varphi'}\begin{pmatrix} 1 & -i \\ -i & -1 \end{pmatrix} - \frac{1}{2}\sin^2\frac{\Gamma}{2}e^{i2(\varphi-\varphi')}\begin{pmatrix} 1 & i \\ -i & 1 \end{pmatrix}$$
$$- \frac{1}{2}\sin^2\frac{\Gamma}{2}e^{-i2(\varphi-\varphi')}\begin{pmatrix} 1 & -i \\ i & 1 \end{pmatrix}$$

There are seven diffracted orders totally. Now, we define the seven orders as $(0, 0)$, $(1, 0)$, $(-1, 0)$, $(0, 1)$, $(0, -1)$, $(1, -1)$ and $(-1, 1)$ in turn. For convenience, $(1, -1)$ and $(-1, 1)$ are written ± 2 orders in this paper.

Absolutely, the PB phase of the second order is $e^{i2(\varphi-\varphi')} = e^{i2\left(\frac{\pi x}{\Lambda} - \frac{\pi x\cos\theta}{\Lambda} + \frac{\pi y\sin\theta}{\Lambda} + \theta\right)}$, so the deflection angle of the second orders ϕ is determined by the grating pitch and the angle between the two grating vectors. And the deflection angle ϕ can be separated into the deflection angle along the x axis ϕ_x and the deflection angle along the y axis ϕ_y. The deflection angles obey the following grating equation:

$$\sin\phi_x = (1 - \cos\theta)\lambda/\Lambda$$

$$\sin\phi_y = \sin\theta\lambda/\Lambda.$$

The effective pitch in xandy axis can be given: $\Lambda_x = \frac{\Lambda}{1-\cos\theta}$ and $\Lambda_y = \frac{\Lambda}{\sin\theta}$. And ϕ can be calculated by the following equation:

$$\phi = \sqrt{\phi_x^2 + \phi_y^2}.$$

When $\theta = \pi/2$, $\phi = \sqrt{2}\phi_x = \sqrt{2}\phi_y$, the deflection angles of the second orders are along the directors of $\pm 45°$ azimuthal angle; when $\theta = \pi$, $\phi_y = 0°$ and $\phi = \phi_x = \arcsin 2\lambda/\Lambda$, the size of the second orders deflection angles is almost twice as the first order and the directors are along x axis. So, the diffraction angles of the 2D polarisation grating can be controlled by the twist angle between the top and bottom substrate and grating pitch.

The diffraction efficiency and polarisation properties of each diffraction order can be given by the vectorial Fourier coefficients of the transmitted field [31]:

$$D_{(m,n)} = \frac{1}{\Lambda_x\Lambda_y}\int_0^{\Lambda_x}\int_0^{\Lambda_y} TEe^{\frac{-i2\pi mx}{\Lambda_x}}e^{\frac{-i2\pi ny}{\Lambda_y}}dxdy$$

The diffraction efficiency of each order is given by $\eta_{(m,n)} = |E|^{-2}|D_{(m,n)}|^2$. Thus, we obtain

$$\eta_{0,0} = \cos^4\frac{\Gamma}{2},$$
$$\eta_{\pm 1, 0} = \frac{1\pm S_3'}{2}\sin^2\frac{\Gamma}{2}\cos^2\frac{\Gamma}{2},$$
$$\eta_{0, \pm 1} = \frac{1\pm S_3'}{2}\sin^2\frac{\Gamma}{2}\cos^2\frac{\Gamma}{2},$$
$$\eta_{(\pm 1,\mp 1)} = \frac{1\pm S_3'}{2}\sin^4\frac{\Gamma}{2},$$

where S_3' is the normalised Stokes parameter denoting the fraction of incident circular polarisation. For left and right circular polarisation, $S_3' = +1$ and -1, respectively. From the transfer matrix we can see that the diffraction properties of the first orders are same as the traditional one dimension polarisation grating. It can also be seen that if $\Gamma = \pi$, all the incident light would be diffracted into ± 2 orders. The transfer matrix of the second orders is much interesting. If the input light is circularly polarised, only one second order will be obtained, and the polarised state is conserved which is different from the conventional polarisation grating. It makes polarisation grating be applied in optical system more flexible. In this manner, a 2D polarisation grating
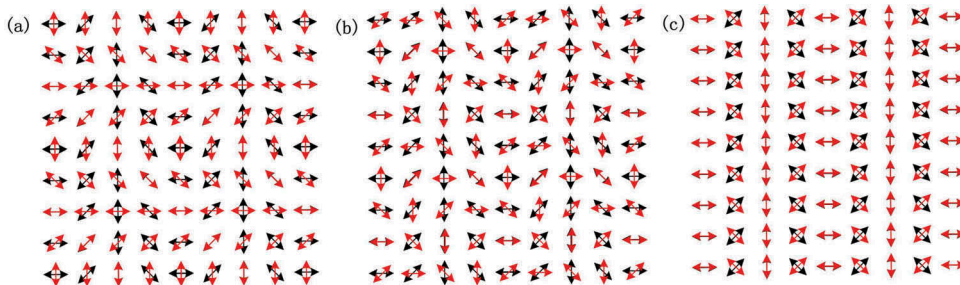

Figure 2. (Color online) LC molecules director distribution with different grating vector angles. (a) θ= π/2, (b) θ= 3/4 π and (c) θ = π.

with 100% diffraction efficiency for a single second order can be accomplished theoretically.

3. Experiments

The fabrication method of our 2D LC polarisation grating is polarisation holography. Polarisation holography involves recording the polarisation distribution of the interference light field of two orthogonal polarised beams into photo-alignment materials. Two coherent beams with orthogonal circular polarisation are superimposed with a small angle, and the spatially rotating linear polarisation distribution is generated, which can be recorded by the photo-alignment materials and makes LC molecules align following the linear polarisation distribution. In the experiment, the 2D LC polarisation grating is consisting of two indium-tin-oxide glass substrates. And both substrates are spin coated with photo-alignment layer (LPP) [32]. The fabrication setup is similar to that used by C. Oh and M. Escuti [33]. And it is described schematically as Figure 3. The HeCd laser (wavelength, $\lambda = 325nm$) is coupled into the hole by the micro-objective, and then collimated by lens. The collimated beam is divided into two beams with the same intensity by the BS. The two beams are reflected by mirrors and pass through the quarter-wave-plates which fast axes are perpendicular to each other, respectively, and finally they overlap on the sample generating a spatially varying linear polarisation distribution. The top and bottom substrates were individually exposed to the periodic spatially rotating linear polarisation pattern with the exposure dose of 5 J/cm^2 as shown in Figure 4. But there is an angle between the grating vectors of the top and bottom substrates. Then, the substrates were assembled together separated by 10 μm spacers. The
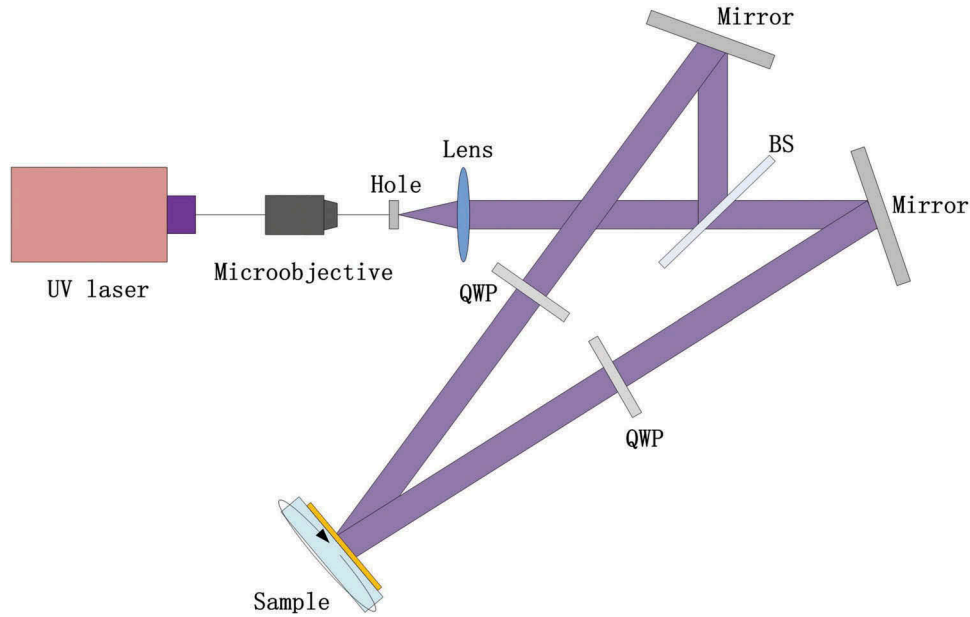

Figure 3. (Color online) The schematic of the optical setup for fabrication. BS, beam splitter; QWP, quarter-wave plate.
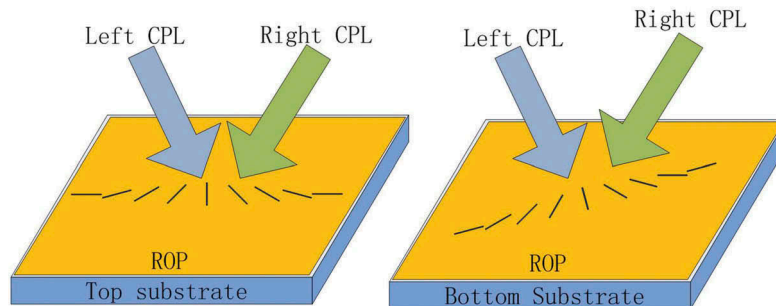

Figure 4. (Color online) The schematic of LC cell exposure progressing.

polarisation grating pitch is 25 μm. Next, the cells were filled by capillary action with the LC mixture Mo16 (from DIC) above the clearing temperature (~120) and slowly cooled down into the nematic phase. Three samples with grating vector angles of $\pi/2$, $3\pi/4$ and π were fabricated in the same manner, respectively.

A He-Ne laser (wavelength, $\lambda_p = 633nm$) was used as probe beam to investigate the diffraction properties of the new-style polarisation grating, as presented in Figure 5. The laser pass through the polariser, quarter wave plate and the sample successively, and then was detected by the detector.
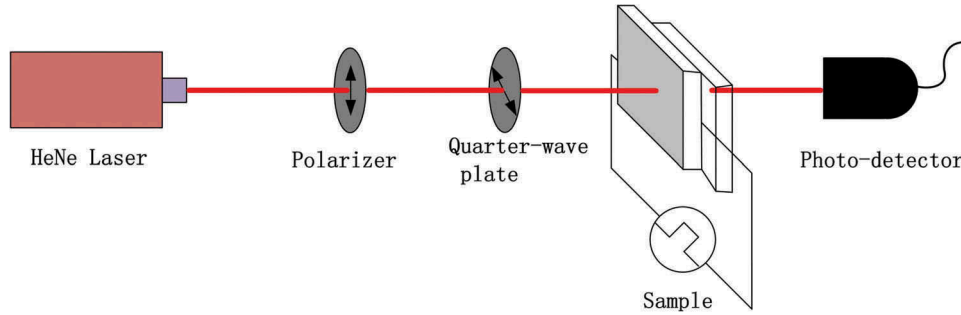

Figure 5. (Color online) Schematic experimental setup for measuring the diffraction characteristics of a PG with a He-Ne laser.
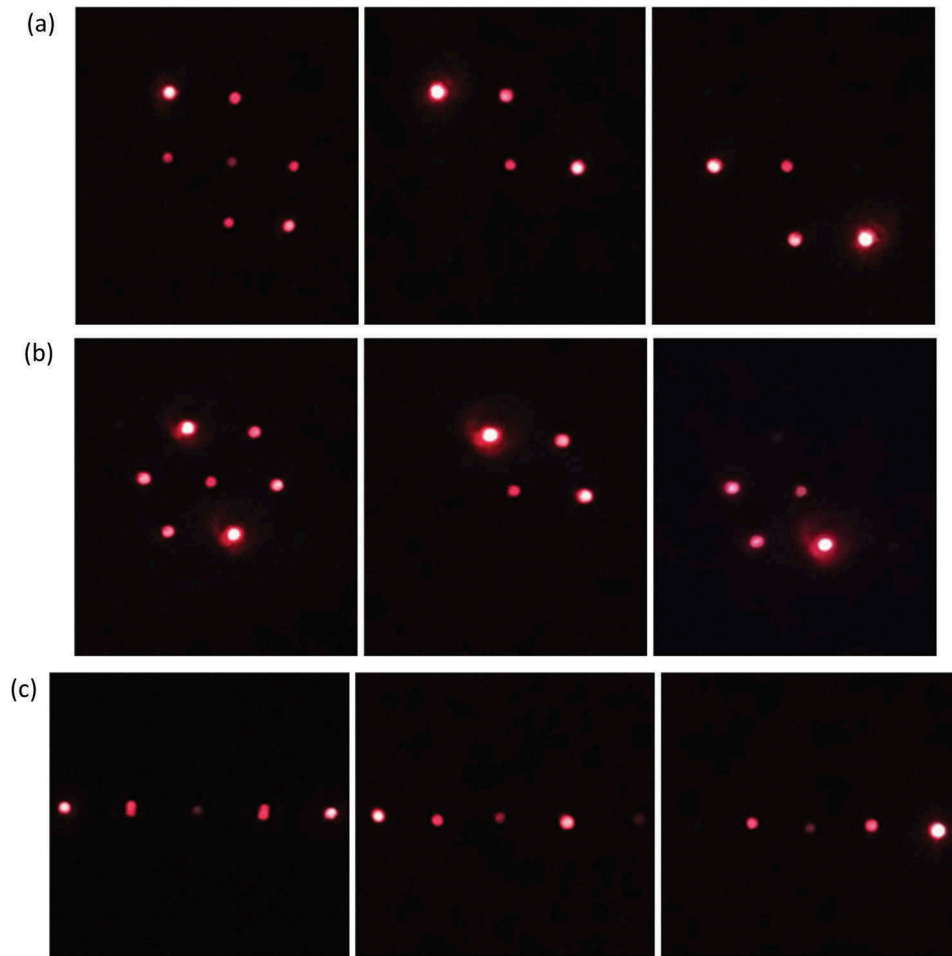

Figure 6. (Color online) Diffraction images for the two-dimensional grating with different crossing angles; (a) θ= π/2, (b) θ= 3/4 π and (c) θ = π.

4. Result and discussion

No detectable diffraction of the probe beam has been observed by the assembled polarisation holograms (empty cells). Diffraction pattern occurred only when the LC was infiltrated in the cell. Figure 6 displays the diffraction patterns of the three formed PG samples with different polarisation incident light. The diffraction patterns of three samples with grating vectors twist angle between the top and bottom substrates of $\pi/2$, $3\pi/4$ and π was shown in Figure 6(a–c), respectively. All the three samples were applied with suitable voltages respectively to make the LC molecular in the middle layer align perpendicularly to the substrates. For every picture in Figure 6, the left pattern respects to linearly polarised incident beam, the middle respects to left circular polarisation (LCP) incidence and the right respects to right circular polarisation (RCP) incidence. The diffraction pattern of $\pi/2$ twist angle was measured under 2.3V applied voltage. The diffraction efficiency of zero, first and second orders are 11.3%, 12.5% and 76.2%, respectively.

In Figure 7, we report the microscope images of $\pi/2$, $3\pi/4$ and π twist angle polarisation gratings under a polarised optical microscope, respectively. These investigations allow to gain insight about the LC molecule director configuration in the bulk. 2D LC structures with crossed defect lines are observed. In Figure 7, the dark areas correspond to the planar nematic regions whose director is parallel or perpendicular with respect to the polariser, while the bright areas correspond to the completely twisted regions where the nematic optical axis at the exit surface is parallel to the analyser. When rotating the analyser, the bright and dark domains interconvert gradually, confirming the continuous varying of the LC directors. This reveals that the designed director distribution is transferred into the twist polarisation gratings.

In fact, the energy distribution in the diffracted beams can be modulated by applying an external voltage to the LC cell. Low external voltage applied to the 2D LC grating uniformly, which provides control of the effective birefringence Δn and allows to properly adjust the diffraction efficiency of the diffraction orders. The electro-optical behaviour of the LC gratings has been investigated measuring the intensities of the diffracted beams versus the ac voltage (f = 1kHz) ramped from $V_{RMS} = 0$ to 10 V. In Figure 8, we report the curve of diffraction efficiency of 0th order, $(+1, 0)$ order and +2 order of the π twist angle polarisation gratings versus voltage V_{RMS}, for left circularly polarised probe beam. As shown in Figure 8, the operation region is divided into three regimes: regime I(V<0.5), II($0.5 \leq V < 1.5$) and III ($V \geq 1.5$). In regime I, retardation is almost constant, resulting in a roughly constant diffraction efficiency because the applied voltage is lower than the threshold voltage of Freedericksz transition. When the applied voltage exceeds 0.5 V (regime II), the LC director distribution of the middle layer is disordered, causing the deterioration of the diffraction properties of the TN-LC grating. When the applied voltage exceeds 1.5 V (regime III), the molecules in the middle plane become almost vertical to the substrate plane. The direction of LC molecular of the upper- and lower-half layers are governed by the photo-alignment direction on the upper and lower surfaces because the LC directors in the mid-plane are reoriented almost vertically. Furthermore, the thick disclinations that deteriorate the diffraction properties disappear desirably because the twist deformation is no longer maintained in the bulk layer. In this regime, the LC cell can be considered as a stack of two hybrid alignment cells with an equal retardation of $\frac{\Gamma}{2}$. When the retardation equals π, the upper- and lower-half layers function as a hybrid alignment LC polarisation grating. The diffraction efficiencies of the second orders reach the maximum values at 1.9 V as shown in Figure 8. If the incident light is circularly polarised, there is only
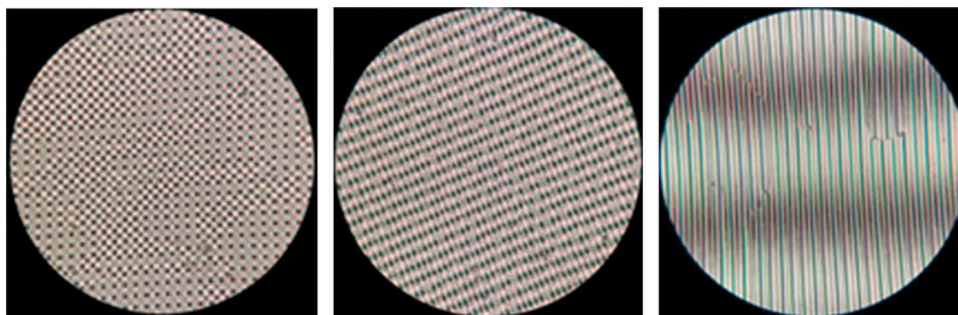

Figure 7. (Color online) The micrograph of two-dimensional polarisation grating with crossing angles of $\pi/2$ (a), $3\pi/4$ (b) and π (c) observed under a polarised optical microscope.
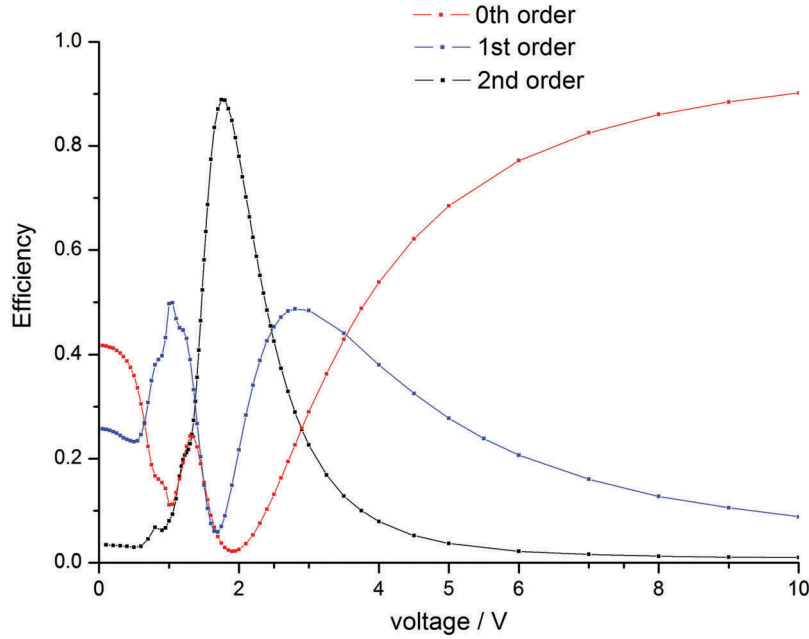
Figure 8. (Color online) The curve of diffraction efficiencies versus the ac voltage (f = 1kHz) of the two-dimensional polarisation gratings. The spots are the data gotten by experimental measure, and the curves are formed by the connection of the spots.

one second order. And the maximum value of diffraction efficiency is up to 90%.

The two sub-layers operate as independent LC polarisation gratings, as mentioned above. Now, we consider the case when RCP light is incident on the LC grating. After passing through the first layer, the light beam is deflected at a certain angle α and the polarisation state is converted into LCP. When the LCP light passes through the second layer, the LCP light is further deflected at an angle of β on the basic of α. Different diffraction pattern can be created by changing the twist angles and the pitches of the lower and upper gratings. Furthermore, because the polarisation state turns into RCP again, the polarisation state is also maintained, which is the same as the theory analysis.

Besides the operation voltage, response time is also an important parameter for LCPG. The rise time and decay time were measured which are 4 and 25ms, respectively. The rise and decay time are defined as the duration time which the efficiency of the 0th order changes from 10% to 90% and from 90% to 10%, respectively. The response time is measured by utilising a 1 kHz signal voltage with intensity alternating between 2 V_{RMs} and 10 V_{RMS}. In the meantime, the second-order intensity converts between the maximum and the minimum. The response time can be further improved by utilising the double frequency LC material or increasing the applied voltage or decreasing the cell thickness.

5. Conclusion

In this paper, we demonstrate a 2D LC polarisation grating which LC molecular alignment director in the top and bottom substrate is different. Low scattering and high efficiency have been achieved. The gratings diffract in different directions with different polarisation states, which can be optically controlled through the polarisation state of the incident light beam. Additionally, the diffraction efficiency of the LC grating exhibits a complicated voltage dependence. When an appropriate voltage is applied, it operates as a stack of two hybrid-orientation-type LC polarisation gratings with different grating vectors. The maximal diffraction efficiency of the second order is up to 90%, when the phase retardation of the LC cell is even times of π. The incident light will all be diffracted into the 0th order as a sufficiently high voltage is applied because the LC molecular orientation becomes homeotropic. Furthermore, the polarisation state is conserved in the 0th order and second order for the circularly polarised incident light. The diffraction properties of the special grating can be designed easily, and the nature of polarisation conservation would be advantageous for more flexible designs of practical optical systems.

sponsored by the National Science Foundation of China (11604327, 61377032, 61378057, 61405194 and 61475152).

Disclosure statement

No potential conflict of interest was reported by the authors.

Funding

References

[1] Chen HW, Lee JH, Lin BY, et al. Liquid crystal display and organic light-emitting diode display: present status and future perspectives. Light Sci Appl. 2018;7(3):17168.

[2] Zhang Z, You Z, Chu D. Fundamentals of phase-only liquid crystal on silicon (LCOS) devices. Light Sci Appl. 2014;3(10):e213.

[3] Nolan DA, Milione G, Leach J, et al. Using the nonseparability of vector beams to encode information for optical communication. Opt Lett. 2015;40(21):4887–4890.

[4] Avci N, Hwang S-J. Electrically tunable polarisation-independent blue-phase liquid crystal binary phase grating via phase-separated composite films. Liq Cryst. 2017;44(10):1559–1565.

[5] Li H, Wang C, Pan Y, et al. Transient holographic grating in azo-dye-doped liquid crystals with off-resonant light. Liq Cryst. 2016;44(6):933–938.

[6] Pancharatnam S. Generalised theory of interference and its applications. Proc Indian Acad Sci A. 1956;44(6):398–417.

[7] Berry MV. Quantal phase factors accompanying adiabatic changes. Proc R Soc London Ser A. 1984;392(1802):45–57.

[8] Tervo J, Turunen J. Paraxial-domain diffractive elements with 100% efficiency based on polarization gratings. Opt Lett. 2000;25(11):785–786.

[9] Provenzano C, Pagliusi P, Cipparrone G. Highly efficient liquid crystal based diffraction grating induced by polarization holograms at the aligning surfaces. Appl Phys Lett. 2006;89(12):2588.

[10] Oh C, Escuti MJ. Numerical analysis of polarization gratings using the finite-difference time-domain method. Phys Rev A. 2007;76(4).

[11] Kim J, Komanduri RK, Lawler KF, et al. Efficient and monolithic polarization conversion system based on a polarization grating. Appl Opt. 2012;51(20):4852–4857.

[12] Kim J, Oh C, Serati S, et al. Wide-angle, nonmechanical beam steering with high throughput utilizing polarization gratings. Appl Opt. 2011;50(17):2636–2639.

[13] Gori F. Measuring Stokes parameters by means of a polarization grating. Opt Lett. 1999;24(9):584–586.

[14] Nicolescu E, Escuti MJ. Polarization-independent tunable optical filters using bilayer polarization gratings. Appl Opt. 2010;49(20):3900–3904.

[15] Chen J, Bos PJ, Vithana H, et al. An electro-optically controlled liquid crystal diffraction grating. Appl Phys Lett. 1995;67(18):2588–2590.

[16] Wu H, Hu W, Hu H, et al. Arbitrary photo-patterning in liquid crystal alignments using DMD based lithography system. Opt Express. 2012;20(20):16684–16689.

[17] Zhou J, Collard DM, Srinivasarao M. Switchable gratings by spatially periodic alignment of liquid crystals via patterned photopolymerization. Opt Lett. 2006;31(5):652–654.

[18] Wen B, Petschek RG, Rosenblatt C. Nematic liquid-crystal polarization gratings by modification of surface alignment. Appl Opt. 2002;41(7):1246–1250.

[19] Nikolova L, Todorov T. Diffraction efficiency and selectivity of polarization holographic recording. Opt Acta. 1984;31(5):579–588.

[20] Miskiewicz MN, Escuti MJ. Direct-writing of complex liquid crystal patterns. Opt Express. 2014;22(10):12691–12706.

[21] Eakin JN, Xie Y, Pelcovits RA, et al. Zero voltage Freedericksz transition in periodically aligned liquid crystals. Appl Phys Lett. 2004;85(10):1671–1673.

[22] Komanduri RK, Escuti MJ. Elastic continuum analysis of the liquid crystal polarization grating. Phys Rev E. 2007;76(2 Pt 1):021701.

[23] Oh C, Escuti MJ. Achromatic diffraction from polarization gratings with high efficiency. Opt Lett. 2008;33(20):2287–2289.

[24] Crawford GP, Eakin JN, Radcliffe MD, et al. Liquid-crystal diffraction gratings using polarization holography alignment techniques. J Appl Phys. 2005;98(12):1671.

[25] Provenzano C, Pagliusi P, Cipparrone G. Electrically tunable two-dimensional liquid crystals gratings induced by polarization holography. Opt Express. 2007;15(9):5872–5878.

[26] Wang M, Li Y, Yokoyama H. Artificial web of disclination lines in nematic liquid crystals. Nat Commun. 2017;8:388.

[27] Nys I, Nersesyan V, Beeckman J, et al. Complex liquid crystal superstructures induced by periodic photo-alignment at top and bottom substrates. Soft Matter. 2018;14(33):6892–6902.

[28] Glazar N, Culbreath C, Li Y, et al. Switchable liquid-crystal phase-shift mask for super-resolution photolithography based on Pancharatnam-Berry phase. Appl Phys Express. 2015;8:116501.

[29] Li S, Liu Y, Liu CJ, et al. Electrically tunable photo-aligned hybrid double-frequency liquid crystal polarisation grating. Liq Cryst. 2018. DOI:10.1080/02678292.2018.1485976

[30] Wei BY, Chen P, Ge SJ, et al. Fast-response and high-efficiency optical switch based on dual-frequency liquid crystal polarization grating. Opt Mater Express. 2016;6(2):597–602.

[31] Tan L, Ho JY, Kwok HS. Extended Jones matrix method for oblique incidence study of polarization gratings. Appl Phys Lett. 2012;101(5):324–490.

[32] Schadt M, Schmitt K, Kozinkov V, et al. Surface-induced parallel alignment of liquid crystals by linearly polymerized photopolymers. Jpn J Appl Phys. 1992;31(7):2155–2164.

[33] Oh C, Kim J, Miskiewicz MN, et al. Fabrication of ideal geometric-phase holograms with arbitrary wavefronts. Optica. 2015;2(11):958–964.